Backstepping observer dedicated to tire cornering stiffness estimation: Application to an All Terrain Vehicle and a farm tractor

Nicolas Bouton[◇], Roland Lenain[◇], Benoit Thuilot[⋆] and Philippe Martinet[○,⋆]

Abstract— **Most of active devices focused on vehicle stability concerns on-road cars and cannot be applied satisfactorily in an off-road context, since the variability and the non-linearities of the tire/ground contact are often neglected. In previous work, a rollover indicator devoted to light ATVs, accounting for these phenomena has been proposed. It is based on the prediction of the lateral load transfer. Such an indicator requires the on-line knowledge of the tire cornering stiffness, initially selected from a ground classes network. In this paper, an adapted backstepping observer, making only use of yaw rate measurement, is designed to improve specifically tire cornering stiffness estimation. Capabilities of such an observer are demonstrated and discussed through both advanced simulations and actual experiments.**

I. Introduction

Light All Terrain Vehicles (ATVs), such as quad bikes, are designed to provide important driveability. The counterpart is their propensity to roll over. This is a serious concern, in view of their growing popularity. For instance, in the U.S.A., the CPSC (Consumer Product Safety Commission, [8]) has reported 7.188 fatal ATV accidents between 1982 and 2003 and has collected a list of 136.700 injuries resulting from the use of ATVs only for the year 2005. The same year, 50 ATV accidents have been listed by a french insurance company [7], only in the agricultural area.

As a result, the development of on-board devices preventing ATVs from rollover situations is encouraged. Several solutions have already been proposed for road vehicles: steering and braking control ([13] and [1]) or Electronic Stability Program (ESP) systems [4] are some examples. However, since car-like vehicles are supposed to move on high grip ground, such devices consider only pseudo-sliding phenomenon with constant tire cornering stiffness. On the contrary, quad bikes are supposed to move on natural ground with variable contact conditions. Therefore, car-like stability devices cannot be directly adapted to ATVs. The aim of our current research is focused on the development of rollover avoidance devices dedicated to ATVs.

The propose device relies on a rollover risk indicator evaluated from the prediction of the lateral load transfer. Since ATVs move on natural ground, the nonlinear behavior of the tire must be taken into account. Therefore, the tire cornering stiffness has to be estimated on-line. A preliminary solution, detailed in [5], relies on a network of several ground classes selected on-line with respect to the ATV yaw rate measured. However, the main drawbacks of this approach are, on the one hand, the required off-line calibration of the ground classes and, on the other hand, the inaccuracy of the algorithm when grip conditions are far from any ground class.

To overcome these negative aspects, an alternative approach, taking benefit from observer theory, is here considered. Some observers have been proposed ([12], [2] and [3]) to obtain an estimation of the tire cornering stiffness. However most of them are using expensive sensors (a Global Positioning System (GPS) and an Inertial Navigation System (INS)) so that key vehicle state variables are available. The light vehicles considered in that paper do not permit to on-board such complex perception systems. As a consequence, this issue is here addressed with a sensor configuration only composed of a gyrometer, a steering angle sensor and a Doppler radar.

This paper is organized as follows: first a simple dynamic model combined with a linear tire model is defined. Then, a preliminary linear yaw rate observer assuming constant tire cornering stiffness has been developed to demonstrate the impossibility to estimate accurately key vehicle state variables when the tire/ground forces are nonlinear. Therefore, a new observer based on a backstepping approach has been designed to estimate the current yaw rate of the vehicle, thanks to the adaptation of a virtual tire cornering stiffness accounting for tire/ground contact non-linearities. Finally, the relevance of the virtual tire cornering stiffness thus obtained is discussed through both advanced simulations and actual experiments.

II. Vehicle modeling

A. Dynamic bicycle model

We are interested in accounting for sliding in vehicle lateral dynamics. Therefore, the vehicle model is based on an Ackermann model [6] extended with sliding parameters, as described in [9] and depicted on Fig.1. Notations used in this paper are listed below:

- G is the vehicle center of gravity,
- L is the vehicle wheelbase,
- a and b are respectively the front and rear half-wheelbases,
- δ is the steering angle,
- v is the linear velocity at the center of the rear axle,
- u is the linear velocity at the center of gravity,
- ψ is the vehicle yaw angle,

◇ Cemagref, 24 av. des Landais, BP 50085, 63172 Aubière Cedex, France
nicolas.bouton and roland.lenain@cemagref.fr
⋆ LASMEA, 24 avenue des Landais , 63177 Aubière Cedex, France
benoit.thuilot@lasmea.univ-bpclermont.fr
○ ISRC - Sungkyunkwan University, Suwon, South Korea
martinet@skku.edu

- β is the global sideslip angle of the vehicle,
- α_r and α_f are respectively the rear and front sideslip angles,
- F_f and F_r are respectively the lateral forces generated on the front and rear tires.

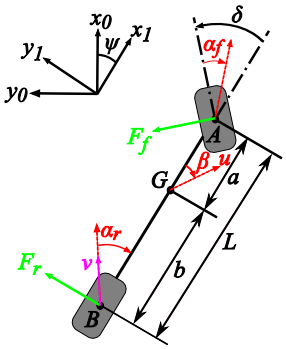

Fig. 1. Dynamic bicyle model with sliding parameters.

B. Lateral forces model

Since sliding parameters and tire/ground forces have been added into the yaw representation of the vehicle, then a tire/ground contact model has to be chosen. Several models permit to describe sliding phenomenon (such as Pacejka model [11]). However such models require numerous and varying parameters. As a consequence, for on-line applications at the considered high velocities, the simpler linear model (1) is here proposed.

$$\left\{ \begin{array}{ll} F_f & = C_f(.)\alpha_f \\ F_r & = C_r(.)\alpha_r \end{array} \right. \tag{1}$$

where $C_f(.)$ and $C_r(.)$ are respectively the rear and front tire cornering stiffnesses, depending on several aspects such as tire normal forces and grip condition variations. In order to take into account the nonlinear behavior of the tire, these tire cornering stiffnesses will be on-line adapted, see III-B.

C. Dynamic equations

Relying on both the linear tire model and the bicycle model representation depicted on Fig.1, motion equations can be derived (as achieved in [9]) by using the fundamental principle of the dynamic. When longitudinal forces and both roll and pitch movements can be neglected (which is realistic here since only lateral vehicle dynamic is studied and described by yaw rate and sideslip angles), motion equations are given by:

$$\left\{ \begin{array}{rcl} \ddot{\psi} & = & \frac{1}{I_z}\left(-aC_f\alpha_f cos(\delta)+bC_r\alpha_r\right) \\ \dot{\beta} & = & -\frac{1}{um}\left(C_f\alpha_f cos(\beta-\delta)+C_r\alpha_r cos(\beta)\right)-\dot{\psi} \\ \alpha_r & = & atan(\beta-\frac{b\dot{\psi}}{u}) \\ \alpha_f & = & atan(\beta+\frac{a\dot{\psi}}{u}-\delta) \\ u & = & \frac{v\cos(\alpha_r)}{\cos(\beta)} \end{array} \right. \tag{2}$$

where I_z and m are respectively the yaw inertial momentum and the mass of the vehicle.

III. Observers design

In this paper three measurements are used to estimate both the yaw rate of the vehicle and the tire cornering stiffness: the steering angle (available from an angle sensor), the yaw rate (from a gyrometer) and the rear axle linear velocity (from a Doppler radar).
The two observers presented in this paper have been developed by considering that the velocity at the vehicle center of gravity is equal to the velocity at the center of the vehicle rear axle (i.e. $u \approx v$). This hypothesis is realistic as long as the global sideslip angle and the rear sideslip angle are relatively small (see (2)), which is generically true for ATVs.

A. Preliminary Linear Observer (LO)

This first observer has been developed under the assumption of constant tire cornering stiffnesses values. It will permit to show the impact of such an hypothesis on the yaw rate observation error with respect to actual grip conditions.

1) State space expression: Assuming that sideslip angles are quite small (less than 10° in practice), equations (2) can be linearized. This leads to the following state space system:

$$\dot{X} = AX + B\delta \tag{3}$$

where $X = (\dot{\psi}\ \beta)^T$, $A = \begin{bmatrix} a_{11} & a_{12} \\ a_{21} & a_{22} \end{bmatrix}$, $B = \begin{bmatrix} b_1 \\ b_2 \end{bmatrix}$ and:
$a_{11} = \frac{-a^2C_f - b^2C_r}{vI_z}$, $a_{12} = \frac{-aC_f + bC_r}{I_z}$, $a_{21} = -\frac{(aC_f - bC_r)}{mv^2} - 1$,
$a_{22} = -\frac{C_r + C_f}{mv}$, $b_1 = \frac{aC_f}{I_z}$, $b_2 = \frac{C_f}{mv}$
Relying on the available measurements, the observation equation is:

$$Y = CX = \begin{bmatrix} 1 & 0 \end{bmatrix} \begin{bmatrix} \dot{\psi} \\ \beta \end{bmatrix} \tag{4}$$

2) Observability: The Kalman observability matrix O can easily be computed:

$$O = \begin{bmatrix} C \\ CA \end{bmatrix} = \begin{bmatrix} 1 & 0 \\ a_{11} & a_{12} \end{bmatrix} \tag{5}$$

According to (5), matrix O is invertible if $a_{12} \neq 0$ which is true as soon as $aC_f \neq bC_r$. It is generally satisfied since $C_r > C_f$ and $b > a$ on most of the quad bikes. Therefore the system is observable.

3) Observer design: Relying on Luenberger observer theory [10], the observer (6) can be proposed:

$$\left\{ \begin{array}{l} \ddot{\widehat{\psi}} = a_{11}\dot{\widehat{\psi}} + a_{12}\widehat{\beta} + b_1\delta + L_1\dot{\widetilde{\psi}} \\ \dot{\widehat{\beta}} = a_{21}\dot{\widehat{\psi}} + a_{22}\widehat{\beta} + b_2\delta + L_2\dot{\widetilde{\psi}} \end{array} \right. \tag{6}$$

with $\widehat{X} = (\dot{\widehat{\psi}}\ \widehat{\beta})^T$ the observer output, $L = \begin{pmatrix} L_1 & L_2 \end{pmatrix}^t$ the observer gain matrix and $\dot{\widetilde{\psi}}$ the yaw rate observation error.
It leads to the two following observation error equations:

$$\left\{ \begin{array}{l} \ddot{\widetilde{\psi}} = (a_{11} - L_1)\dot{\widetilde{\psi}} + a_{12}\widetilde{\beta} \\ \dot{\widetilde{\beta}} = (a_{21} - L_2)\dot{\widetilde{\psi}} + a_{22}\widetilde{\beta} \end{array} \right. \tag{7}$$

The stability of the observer can be demonstrated by considering the Lyapunov function candidate $V_1(\widetilde{X}) = \frac{1}{2}(\dot{\widetilde{\psi}}^2 + \widetilde{\beta}^2)$. Relying on (7), the time derivative of V_1 is:

$$\dot{V}_1 = ((a_{11} - L_1)\dot{\widetilde{\psi}} + a_{12}\widetilde{\beta})\dot{\widetilde{\psi}} + ((a_{21} - L_2)\dot{\widetilde{\psi}} + a_{22}\widetilde{\beta})\widetilde{\beta} \quad (8)$$

Then, if the observer gain L_2 is set to $L_2 = a_{12} + a_{21}$, the time derivative of V_1 is:

$$\dot{V}_1 = (a_{11} - L_1)\dot{\widetilde{\psi}}^2 + a_{22}\widetilde{\beta}^2 \quad (9)$$

According to their definition, the two coefficients a_{11} and a_{22} are strictly negative (since C_f and C_r are strictly positive). As a consequence, if the observer gain L_1 is strictly positive, the time derivative of V_1 is strictly negative. This ensures the asymptotic stability of the observer state.
Moreover, the choice of a large observer gain L_1 ensures the observer robustness even when L_2 is slightly different from its expected value equal to $a_{12} + a_{21}$, (which is always the case in practice).

4) Simulation results: A bicycle model has been simulated with MATLAB software. This model is the same than the one depicted on Fig.1 and includes a Pacejka tire/ground model. The quad bike parameters for the simulations are listed in Table I.

TABLE I
QUAD BIKE PARAMETERS USED IN SIMULATION

Yaw momentum of inertia I_z	130 kg.m^2
Half-front wheelbase a	0.6 m
Half-rear wheelbase b	0.7 m
Quad bike weight m	250 kg

The linear observer (hereafter noted LO) has been developed by considering that the tire stiffnesses are known and have a constant value. A simulation test has been performed to investigate how LO is inaccurate when these assumptions are no longer satisfied. During this simulation, sharp changes are imposed to the velocity and to the steering angle, as depicted on Fig.2. The steady state values for these two variables are respectively 36 km.h^{-1} and 12°. In view of the ground contact parameters, the tire/ground lateral forces enter into the nonlinear area at time $t = 2$s.

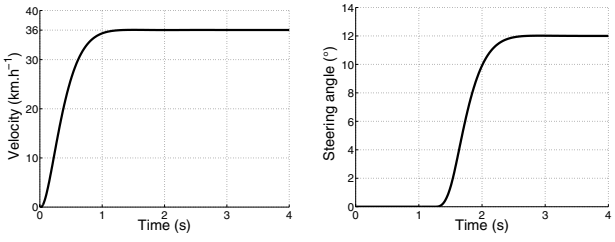

(a) Velocity. (b) Steering angle.

Fig. 2. Velocity and steering angle imposed.

Fig.3 shows the estimated yaw rate supplied by the linear observer when $L_2 = a_{12} + a_{21}$ and $L_1 = 100$.

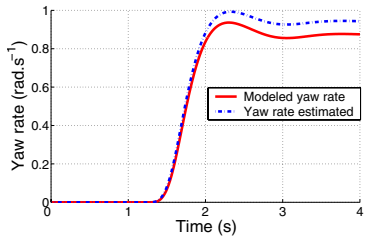

Fig. 3. Yaw rate estimation results with Linear observer.

As expected, it can be checked that, in the pseudo-sliding area ($t < 2s$), when the tire cornering stiffness value used in LO is equal to the actual one ($C_0 = 20.000$ N.rad^{-1}), the yaw rate is satisfactorily estimated. This is no longer the case, beyond $t = 2$s, where the tire/ground contact enters into the nonlinear area.
Therefore, in such situations, the future yaw rate cannot be accurately predicted and our rollover risk indicator based on the prediction of the lateral load transfer of the vehicle would be erroneous, as pointed out in [5].
As a consequence, the tire cornering stiffness has to be online adapted. A first solution could consist in using both a tire stiffness adaptation law and the linear observer. Unfortunately, it would require the measurement of both the yaw rate and the global sideslip angle of the vehicle, however, the latter one is not available with our sensor configuration. Consequently, an adapted backstepping observer is proposed below to estimate the tire cornering stiffness even when tire/ground forces are nonlinear.

B. Adapted backstepping Observer (ABO)

1) Principle: When the tire cornering stiffness is considered as constant (noted C_0 on Fig. 4), the linear tire/ground contact model (1) is only able to describe the pseudo-sliding area of the tire. However, since quad bike are expected to move on slippery ground, tire/ground forces are highly nonlinear. The approach proposed in that paper to satisfactorily estimate lateral forces even in the nonlinear area consists in updating a virtual tire cornering stiffness $C_{estimated}$ as it is depicted on Fig. 4.
Since only one measurement is available to estimate tire ground stiffnesses, the front tire cornering stiffness (C_f) and the rear one (C_r) are assumed to be equal to a global tire cornering stiffness, hereafter noted $C_{estimated}$. In view of (5), the system is still observable if $a \neq b$, which is true for most of the vehicles.

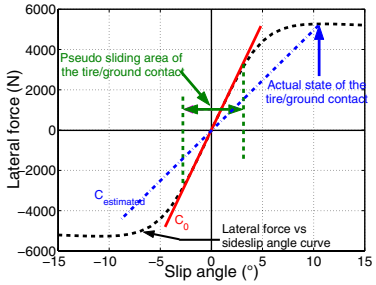

Fig. 4. Estimation principle of the tire cornering stiffness.

2) Backstepping design: The main idea is to design the observation algorithm using a backstepping approach. Let us write the observer equations as follows:

$$\begin{cases} \dot{\hat{\dot{\psi}}} = a_{11}\hat{\dot{\psi}} + a_{12}\hat{\beta} + b_1\delta \\ \dot{\hat{\beta}} = a_{21}\hat{\dot{\psi}} + a_{22}\hat{\beta} + b_2\delta \end{cases} \tag{10}$$

The first step in the observation algorithm consists in ensuring the convergence of the yaw rate observer error ($\tilde{\dot{\psi}} = \dot{\psi} - \hat{\dot{\psi}}$) to zero by treating $\hat{\beta}$ as a control input and by designing this variable in order to impose the following dynamics:

$$\dot{\tilde{\dot{\psi}}} = K\tilde{\dot{\psi}}, \qquad K < 0 \tag{11}$$

The control law expression $\overline{\beta}$ for the intermediate control variable $\hat{\beta}$ can easily be obtained by injecting (11) into the first equation of system (10):

$$\dot{\tilde{\dot{\psi}}} = \ddot{\psi} - \dot{\hat{\dot{\psi}}} = \ddot{\psi} - K\tilde{\dot{\psi}} = a_{11}\hat{\dot{\psi}} + a_{12}\hat{\beta} + b_1\delta \tag{12}$$

This expression suggests to choose $\overline{\beta}$ as:

$$\overline{\beta} = \frac{\ddot{\psi} - K\tilde{\dot{\psi}} - a_{11}\hat{\dot{\psi}} - b_1\delta}{a_{12}} \tag{13}$$

where $\ddot{\psi}$ is the numerical derivative of the measured yaw rate $\dot{\psi}$.
With such a choice, the dynamics of the observed yaw rate is now provided by:

$$\dot{\hat{\dot{\psi}}} = a_{11}\hat{\dot{\psi}} + a_{12}\overline{\beta} + b_1\delta \tag{14}$$

Injecting (14) into (3) leads to the following dynamics for the yaw rate observed error:

$$\dot{\tilde{\dot{\psi}}} = \ddot{\psi} - \dot{\hat{\dot{\psi}}} = a_{11}\tilde{\dot{\psi}} + a_{12}\left(\beta - \overline{\beta}\right) \tag{15}$$

In view of (11), it can be deduced from (15), that:

$$\lim_{t \to +\infty} \overline{\beta} = \beta \tag{16}$$

As a consequence, the virtual control $\overline{\beta}$ appears as a virtual measurement of the global sideslip angle β, to be reached by $\hat{\beta}$. Therefore, the second step consists in achieving this convergence by relying on the global tire cornering stiffness $C_{estimated}$, since the $\hat{\beta}$ dynamics depends on this parameter (via the a_{ij} coefficients), $C_{estimated}$ is then treated as a control input and designed to impose (17):

$$\dot{\tilde{\beta}} = G\tilde{\beta} \tag{17}$$

with $\tilde{\beta} = \overline{\beta} - \hat{\beta}$ and $|G| << |K|$ in such a way that $\tilde{\dot{\psi}}$ decreases faster than $\tilde{\beta}$. The control law expression for $C_{estimated}$ can be obtained by injecting the second equation of (10) and (13) into (17):

$$\dot{\tilde{\beta}} = G\tilde{\beta} = \dot{\overline{\beta}} - \dot{\hat{\beta}} = \frac{a_{11}}{a_{12}}\dddot{\psi} + a_{21}\dot{\hat{\dot{\psi}}} + a_{22}\dot{\hat{\beta}} + b_2\dot{\delta} \tag{18}$$

Terms $\psi^{(3)}$, $\dddot{\hat{\psi}}$ and $\dot{\delta}$ have been neglected in $\dot{\overline{\beta}}$ expression shown in (18) since they are small. Moreover, $\ddot{\hat{\psi}}$ has been replaced by $\ddot{\psi}$ since $\ddot{\tilde{\psi}}$ decreases faster than $\tilde{\beta}$.
Then, by expanding the a_{ij} coefficients according to (3), it can be obtained from (18) the following expression for $C_{estimated}$:

$$C_{estimated} = \frac{\dot{\hat{\dot{\psi}}} - G\tilde{\beta} - \left(\frac{a^2+b^2}{v(a-b)}\right)\ddot{\psi}}{f(\hat{\dot{\psi}}, \hat{\beta}, \delta)} \tag{19}$$

where, $f(\hat{\dot{\psi}}, \hat{\beta}, \delta)$ is given by:

$$f(\hat{\dot{\psi}}, \hat{\beta}, \delta) = \frac{(b-a)\hat{\dot{\psi}}}{mv^2} - \frac{2\hat{\beta}}{mv} + \frac{\delta}{mv} \tag{20}$$

In view of (20), the estimation of the global tire cornering stiffness is properly defined as soon as $v \neq 0$.

3) Simulations results: So as to compare the adapted backstepping observer (hereafter noted ABO) with the LO, the same velocity and steering angle inputs than those depicted on Fig. 2 have been used. The ABO gains have been chosen as $K = -50$ and $G = -5$.

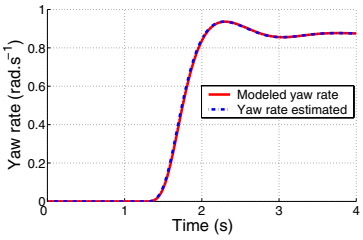

Fig. 5. Yaw rate estimation results with Backstepping observer.

Contrary to Fig. 3, it can be observed on Fig. 5 that the yaw rate estimated with the ABO is satisfactorily superposed with the simulated one. This demonstrates the capabilities of the proposed observer.

IV. Results

In this section, two sets of experimental results are reported. The first ones have been performed by using the multibody simulation software Adams. Indeed, with this software, a virtual quad bike, depicted on Fig. 6(a), has been built using the parameters listed in Table I.
The second set of experiments has been performed with an Ares 640 farm tractor, manufactured by CLAAS and depicted on Fig.6(b). The vehicle parameters are: 14.977 kg.m^2 for the yaw moment of inertia, 1.35 m and 1.51 m for respectively the front and rear half wheelbases and 7.560 kg for the farm tractor weight.

(a) Virtual quad bike. (b) Ares 640.

Fig. 6. Vehicles used for advanced experiments.

A. Simulations results with Adams software

In these simulations, sliding phenomenon has been introduced at the tire/ground contact. The rear axle velocity, the yaw rate and the steering angle have been recorded by Adams with a 100 Hz frequency (identical to the gyrometer one).

1) Path followed: The path followed by the vehicle, depicted on Fig. 7, is composed of a straight line in order for the vehicle to reach a 21 km.h^{-1} constant velocity. Then, two curves have to be described with a steering angle value at 5° for the first one and 10° for the second one.

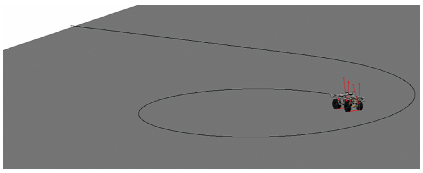

Fig. 7. Quad bike simulation path.

2) Observer results: The two gains of the ABO have been set to $K = -50$ and $G = -5$. Moreover, the observation algorithm is activated only when the steering angle value is beyond 5° in order to avoid non-observable neutral steer situations. In this simulation run, ABO algorithm is then activated at the beginning of the first curve.

On Fig. 8(a), one can check the accuracy of the ABO for the estimation of the yaw rate simulated on Adams: during each bend (between $t = 8$s-13s and $t = 13$s-18s) the yaw rate observation error converges to zero. In order to satisfactorily estimate the vehicle yaw rate, the global tire stiffness has been adapated, as it is depicted on Fig. 8(b).

Several initial values of the tire stiffness have been considered $C_{init1} = 5.000$ N.rad^{-1}, $C_{init2} = 50.000$ N.rad^{-1} and $C_{init3} = 100.000$ N.rad^{-1}. It can be noticed that the initial value has no impact on the estimated tire cornering stiffness supplied by the algorithm: the three curves are superposed.

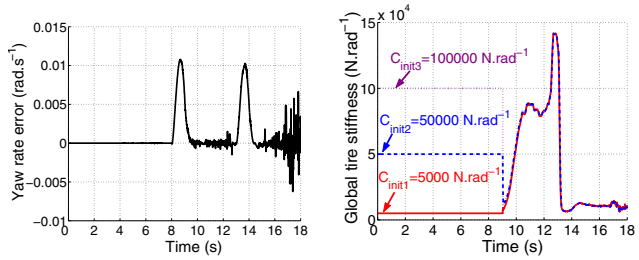

(a) Yaw rate error. (b) Tire stiffness adaptation.

Fig. 8. Observation results with Adams simulation.

Finally, on Fig. 9, the lateral forces measured with Adams have been compared between $t = 8$s and $t = 18$s to the estimated ones by ABO and LO when the initial value of the tire stiffness is set to 50.000 N.rad^{-1}.

Firstly, it can be noticed that during the first curve, since sliding phenomenon is not very important, the estimation of the lateral forces computed either from LO or ABO are both accurate.

During the second curve (between $t = 13$s and $t = 18$s), where sliding is increased, the lateral forces computed from LO (that assumes a constant tire cornering stiffness) are no longer relevant. On the contrary, thanks to the tire cornering stiffness adaptation, the lateral forces computed from ABO stay close to the measured ones. The transient overshoots that can be noticed on Fig. 8(a) for yaw rate and on Fig. 9 for lateral forces correspond to the observer settling time.

The estimated value of the global tire cornering stiffness, supplied by ABO, is then meaningful in order to predict both the yaw rate and the lateral load transfer of the vehicle and can then reliably be used in order to compute a rollover risk indicator such as detailed in [5].

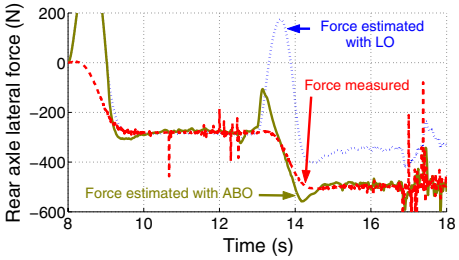

(a) Rear axle lateral force.

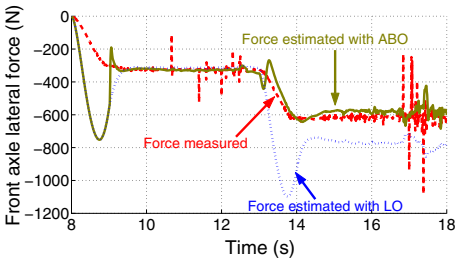

(b) Front axle lateral force.

Fig. 9. Rear and front lateral forces measured and estimated.

B. Actual experimental results

1) Path followed: The path followed by the tractor, depicted on Fig. 10, has been recorded by a RTK GPS sensor. It is composed of a straight line, then a constant curve, and finally another straight line. This maneuver has been performed at a 7 km.h^{-1} constant speed.

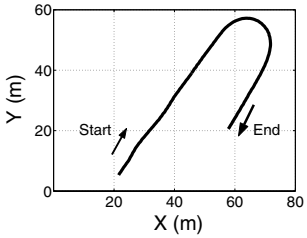

Fig. 10. Path followed by the farm tractor.

2) Observer results: In this case, the frequency of the different sensors is 10 Hz. As a result, the two gains of the ABO have to be decreased and are set to $K = -10$ and $G = -0.1$. The initial values of the global tire cornering stiffness have successively been set to $C_{init1} = 20.000$ N.rad^{-1}, $C_{init2} = 50.000$ N.rad^{-1} and $C_{init3} = 100.000$ N.rad^{-1}.

Fig. 11(a) shows the yaw rate estimated from the ABO compared to the yaw rate measured by the gyrometer. As it has already been noticed in the advanced simulations, the two signals are satisfactorily superposed.
Fig. 11(b) presents the global tire cornering stiffness estimated with the three initial values C_{init1}, C_{init2} and C_{init3}. It can be observed that, during the curve, independently from the initial value, the tire cornering stiffness is adapted in order to reflect the actual tire/ground contact condition.

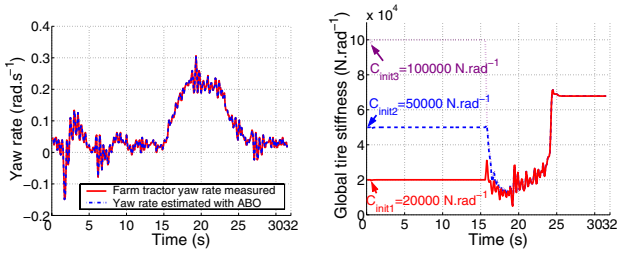

(a) Yaw rate error. (b) Tire stiffness adaptation.

Fig. 11. Observation results with farm tractor.

Finally, since the tractor is equipped with a RTK GPS sensor, the global sideslip angle can be a posteriori calculated. This signal is depicted on Fig. 12 and compared to the global sideslip angles estimated from LO ($C_0 = 100.000$ N.rad^{-1}) and from ABO. It can be noticed that, the one estimated from ABO is correctly superposed with the measured one, even during the curve when it is not the case with the estimation supplied by LO. This shows the relevancy of the adaptation algorithm during this part of the trajectory.

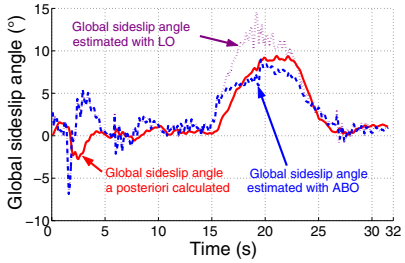

Fig. 12. Global sideslip angle estimation result.

V. Conclusion and Future Work

A. Conclusion

This paper proposes an adapted backstepping observer (ABO) to estimate the global tire cornering stiffness from yaw rate observation. It is expected to be used to supply on-line relevant values to a rollover risk indicator dedicated to off-road vehicles. A dynamic bicycle model, as well as a tire/ground description have been detailed. Based on these representations, a preliminary linear yaw rate observer (LO) has been developed under the assumption that the tire cornering stiffness is constant. It has then been shown that the observed yaw rate error does not longer converge to zero as soon as tire/ground forces enter into nonlinear area. This points out the necessity of adapting on-line the tire cornering stiffness in order to accurately predict the vehicle behavior in such situations. This is the aim of the backstepping observer proposed in this paper (ABO). It has been designed according to two steps. In the first one the yaw rate is estimated from a virtual measurement of the global sideslip angle. In the second step a global tire cornering stiffness is adapted in order that the estimated global sideslip angle value fits with this virtual measurement. Then, the relevance of this approach has been investigated through both advanced simulations on a virtual ATV and actual experiments on a farm tractor.

B. Future work

The validation of the algorithm proposed in this paper has to be continued on an actual all terrain vehicle. The equipment and calibration of an experimental light ATV is under initiation to confirm the promising results here presented. The extension of the proposed work to additionnal sensors is furthermore investigated. In particular, the use of further measurements could permit to improve the estimation of the global sideslip angle and consequently the estimation of the global tire cornering stiffness.
The on-line adaptation of tire cornering stiffness offers a relevant input to address ATV stability. Our main research work aims at designing on-board devices for rollover avoidance based on a stability criterion. Such systems are intended to be designed relying on constrained, optimal and predictive control principles.

References

[1] J. Ackermann and D. Odenthal. Advantages of active steering for vehicle dynamics control. In *Intern. Conf. on Advances in Vehicle Control and Safety (AVCS)*, Amiens, France, 1998.

[2] R. Anderson and D.M. Bevly. Estimation of slip angles using a model based estimator and GPS. In *American Control Conference (ACC)*, Boston, U.S.A., 2004.

[3] R. Anderson and D.M. Bevly. Estimation of tire cornering stiffness using GPS to improve model based estimation of vehicle states. In *IEEE Intelligent Vehicles conference (IV)*, Las Vegas, U.S.A., 2005.

[4] R. Bosch. *Safety, comfort and convenience systems*. Wiley, Hoboken, U.S.A., 2006.

[5] N. Bouton, R. Lenain, B. Thuilot, and J-C. Fauroux. A rollover indicator based on the prediction of the load transfer in presence of sliding: application to an all terrain vehicle. In *Intern. Conf. on Robotics and Automation (ICRA)*, Rome, Italia, 2007.

[6] C. Canudas de Wit, B. Siciliano, and G. Bastin. *Theory of robot control*. Springer Verlag, 1996.

[7] CCMSA. Accidents du travail des salariés et non salariés agricoles avec des quads. Technical report, Observatoire des risques professionels et du machinisme agricole. Paris, France, 2006.

[8] U.S. Consumer Product Safety Commission. 2005 annual report of ATV deaths and injuries. Technical report, CPSC annual report. Washington DC, U.S.A., 2006.

[9] R. Lenain. *Contribution à la modélisation et à la commande de robots mobiles en présence de glissement*. PhD thesis, Clermont-Ferrand University, France, 2005.

[10] T. Meurer, K. Graichen, and Gilles E.D. *Control and observer design for nonlinear finite and infinite dimensional systems*. Springer Verlag, Berlin, Germany, 2005.

[11] H. B. Pacejka, E. Bakker, and L. Nyborg. Tyre modelling for use in vehicle dynamics studies. *SAE Paper*, (870421), 1987.

[12] J. Ryu and J. Christian Berges. Vehicle sideslip and roll parameter estimation using GPS. In *6th Int. Symp. on Advanced Vehicle Control (AVEC)*, Hiroshima, Japan, 2002.

[13] B. Schofield. Vehicle dynamics control and controller allocation for rollover prevention. In *15th IEEE Conference on Control Applications (CCA)*, Munich, Germany, 2006.